Biochemical and Biophysical Research Communications 424 (2012) 771–776

Contents lists available at SciVerse ScienceDirect

Biochemical and Biophysical Research Communications

journal homepage: www.elsevier.com/locate/ybbrc

Tyrosine B10 triggers a heme propionate hydrogen bonding network loop with glutamine E7 moiety

Brenda J. Ramos-Santana, Juan López-Garriga *

Department of Chemistry, University of Puerto Rico, Mayagüez Campus, P.O. Box 9019, Mayagüez 00681-9019, Puerto Rico

ARTICLE INFO

Article history:
Received 4 July 2012
Available online 15 July 2012

Keywords:
Lucina pectinata
Hemoglobin I (HbI)
Cyanide-ligated ferric hemoglobin I (HbICN)
Tyrosine (Tyr)
Glutamine (Gln)
Nuclear overhauser effect (NOE)
Two-dimensional nuclear overhauser effect spectroscopy (NOESY)

ABSTRACT

Propionates, as peripheral groups of the heme active center in hemeproteins have been described to contribute in the modulation of heme reactivity and ligand selection. These electronic characteristics prompted the question of whether the presence of hydrogen bonding networks between propionates and distal amino acids present in the heme ligand moiety can modulate physiological relevant events, like ligand binding association and dissociation activities. Here, the role of these networks was evaluated by NMR spectroscopy using the hemoglobin I PheB10Tyr mutant from *Lucina pectinata* as model for TyrB10 and GlnE7 hemeproteins. ^{1}H-NMR results for the rHbICN PheB10Tyr derivative showed chemical shifts of TyrB10 OHη at 31.00 ppm, GlnE7 $N_{\varepsilon 1}H/N_{\varepsilon 2}H$ at 10.66 ppm/−3.27 ppm, and PheE11 $C_{\delta}H$ at 11.75 ppm, indicating the presence of a crowded, collapsed, and constrained distal pocket. Strong dipolar contacts and inter-residues crosspeaks between GlnE7/6-propionate group, GlnE7/TyrB10 and TyrB10/CN suggest that this hydrogen bonding network loop between GlnE7, TyrB10, 6-propionate group, and the heme ligand contribute significantly to the modulation of the heme iron electron density as well as the ligand stabilization mechanism. Therefore, the network loop presented here support the fact that the electron withdrawing character of the hydrogen bonding is controlled by the interaction of the propionates and the nearby electronic environments contributing to the modulation of the heme electron density state. Thus, we hypothesize that in hemeproteins with similar electrostatic environment the flexibility of the heme-6-propionate promotes a hydrogen bonding network loop between the 6-propionate, the heme ligand and nearby amino acids, tailoring in this way the electron density in the heme-ligand moiety.

1. Introduction

Heme groups characterize the active center of proteins such as the globins, cytochromes, and peroxidase [1]. In these proteins the heme iron serves as a source or sink of electrons during electron transfer or redox chemistry [2], oxygen (O_2) transport or storage, and as a gas sensor [2–4]. In essence, peripheral side groups of the heme, such as vinyl and propionate side chains have simply been considered as anchors for connecting the heme prosthetic group to the protein matrix [5]. It has been reported that in cytochrome P450 the heme-6 and 7-propionate side chains form hydrogen bonding interactions with nearby amino acids [6]. Nevertheless, the role of the hydrogen bonding network between the 6 and 7- propionate heme groups, and the distal residues in heme-protein ligand binding, dissociation and stabilization mechanisms remains unclear. Here, we have investigated the possible inherent role of heme propionate groups in the active center of the rHbICN PheB10Tyr mutant from the clam *Lucina pectinata* using NMR spectroscopy.

This invertebrate clam contains three hemoglobins, HbI, HbII and HbIII, each one with diverse function. HbI is responsible for the delivery of H_2S to intracellular symbiotic bacteria that comprises about one third of the volume of *L. pectinata* gill [7]. HbI is considered a sulfide-reactive monomeric protein of 142 amino acid residues with an active site composition that involves three Phe's at B10, CD1 and E11 positions and a Gln at the E7 position [8,9]. The natural replacement of HisE7, common in globins, by GlnE7 and the exclusive aromatic arrangement of phenylalanine residues illustrate how the unique distal environment in HbI might influence ligand interactions with the heme. For instance, the fast association of H_2S for HbI, $k_{on} = 2.3 \times 10^5\ M^{-1}\ s^{-1}$, and its slow dissociation, $k_{off} = 0.22 \times 10^{-3}\ s^{-1}$, are responsible for the high affinity of ferric HbI for H_2S, which is 4000-fold greater than those of ferric HbII, HbIII and myoglobin [10]. HbI also exhibits one of the fastest known O_2 association ($k_{on} = 100–200\ \mu M^{-1}\ s^{-1}$) and dissociation ($k_{off} = 61\ s^{-1}$) rates [10]. HbI differ from HbII in that the

* Corresponding author. Fax: +1 787 265 5476.
E-mail addresses: brenda.ramos@upr.edu (B.J. Ramos-Santana), juan.lopez16@upr.edu (J. López-Garriga).

0006-291X/$ - see front matter © 2012 Elsevier Inc. All rights reserved.
http://dx.doi.org/10.1016/j.bbrc.2012.07.032

former has a Phe instead of a Tyr at the B10 position. Site-directed mutagenesis studies suggested that the HbI PheB10Tyr mutant exhibits kinetics and structural properties similar to HbII [11]. Interestingly, the TyrB10 and the GlnE7 residues appear in the truncated hemoglobins (trHbs) [12]. Like HbII, most of the examined trHbs exhibit very high O_2 affinities due to unusual slow dissociation rates. This slow oxygen off rates has been suggested to be a consequence of a strong hydrogen bonding between the GlnE7 and TyrB10 with the bound ligand [13]. A hydrogen bonding network has also been invoked for the stabilization of O_2 in HbII [14]. The crystal structure of $HbIIO_2$ shows a dimeric structure and a small heme pocket cavity inducing the formation of strong H-bond between the iron and the oxygen molecule, where oxygen is anchored to the heme through hydrogen bonds with TyrB10 and GlnE7 stabilizing in turn the heme (Fe^{II}) oxidation state [15]. It has been proposed that this network is responsible for the slow oxygen off rate in HbII, similar to the *Ascaris suum* hemoglobin that also has a GlnE7 and TyrB10 on the distal heme pocket [14]. Furthermore, the crystal structure of $HbIIO_2$ shows a hydrogen bonding network in the heme proximal site between the HisF8 nitrogen proton, and a water molecule, which forms a H-bond with the heme 7-propionate group [15]. It has been suggested that this proximal network modulate the His98 trans-effect, affecting the oxygen dissociation rate. Similarly, NMR studies of the proximal site of deoxygenated horse heart myoglobin suggests that replacement of the heme-7-propionate with a methyl group slightly weakens the His-93-heme iron bond [16].

Herein, the CN binding and stability in the heme pocket of the rHbI PheB10Tyr mutant allowed the identification of three side chain labile protons (OH_η, $N_{\varepsilon1}H$, $N_{\varepsilon2}H$) for the distal residues TyrB10 and GlnE7 by isotopic behavior at 31.00, 10.66, and −3.27 ppm, respectively. Their relaxation time, T_1, (OH_η at 14 ms, $N_{\varepsilon1}H$ at 25 ms), dipolar shift, and NOE effects to adjacent residues were used to place the distal residues in the heme moiety. The large NOE from the GlnE7 $N_{\varepsilon2}H$ and dipolar contact with the $6H_{\beta's}$ propionate group at 0.20 and −1.40 ppm indicate that this residue is very close to the heme iron and the bound ligand. Saturation of the $B10OH_\eta$ peak results in a strong NOE to a proton near 6.46 ppm which is assigned to $GlnE7C_{\gamma1}H$. In addition, the results show that TyrB10 adopts a proper orientation to allow a strong H-bond with the bound cyanide. The results also indicate that: (a) the PheB10Tyr mutation promotes an H-bonding network loop through conformational changes of heme pocket, (b) the propionate group H-bonding network restricted the flexibility of prosthetic group, and (c) the hydrogen bonding interactions between distal amino acids, ligand, and propionate groups modulate the electron density of the iron and facilitates heme-ligand stabilization. Similar interaction can be suggested for oxy-heme complexes with analogous heme distal center, like HbII and HbIII from *L. pectinata* or trHbs [12], where the hydrogen bonding network can modulate heme-O_2 affinity and chemistry.

2. Materials and methods

Expression and culture growth of the rHbI PheB10Tyr mutant was prepared and purified as previously reported [17]. Ferric rHbI PheB10Tyr mutant was prepared by a 1:1 oxidation reaction as described previously [18]. Cyanide rHbI PheB10Tyr complex was obtained by titration of the ferric rHbI PheB10Tyr mutant with a 200 mM NaCl/20 mM NaCN solution prepared with ^1H_2O(90%)/^2H_2O(10%) or ^2H_2O (100%). The formation of the cyanide derivative was monitored by its characteristic optical spectra [19]. 1D and 2D ^{1}H-NMR spectra were collected on Bruker spectrometers operating at 600 MHz with pulse sequences and acquisition parameters previously described in the literature [20,21].

3. Results

Fig. 1 compares the ^{1}H-NMR spectra of the rHbICN PheB10Tyr variant in ^1H_2O (1A) and ^2H_2O (1B). Comparison of these spectra reveals the presence of three strongly relaxed labile protons at 14.86, 31.00 and −3.27 ppm assigned to the axial proximal residue HisF8 $N_{\delta1}H$, and distal residues $TyrB10OH_\eta$ and GlnE7 $N_{\varepsilon2}H$, respectively. Fig. 1C shows the 1D NOE spectrum upon saturation of the $TyrB10OH_\eta$ peak at 31.00 ppm. It is characterized by a short longitudinal-relaxation time (T1) at approximately 14.0 ms with diverse NOE to TyrB10 ring protons ($C_\varepsilon H$ and $C_\delta H$), GlnE7 side chain ($C_{\beta1}H$, $C_{\beta2}H$, $C_{\gamma1}H$, $C_{\gamma2}H$), and PheE11 ring protons (N_pH, $C_{\beta1}H$ and $C_{\beta2}H$). Significantly, no NOE to GlnE7 $N_{\varepsilon1}H$ and GlnE7 $N_{\varepsilon2}H$ was observed, showing strong decoupling among these protons. The assignments were based on the presence or absence of the isotopic proton and by comparing the values of the axial conserved residue and the heme peripheral groups including methyl, vinyl and propionate protons as reported in the literature [1,21]. For example, the pyrrole 1-CH_3 and 5-CH_3 methyl groups have been observed in the ^{1}H-NMR spectra of hemoglobins and myoglobins in the 30.00–17.00 ppm downfield region. On the other hand, the 19.90 ppm chemical shift has been assigned to the 6-$H_{\alpha'}$ propionate group, while the chemical shifts at 19.40, −6.10 and −7.99 ppm have been designated to a 2-H_α/$H_{\beta t}$/$H_{\beta c}$ vinyl group, respectively. These heme hyperfine shifts patterns have been reported for hemoproteins active in both diamagnetic and paramagnetic region, specifically in six coordinated heme complexes with low spin, Fe(^{III}) oxidation, and ½ spin state configuration [1]. The pattern of heme chemical shifts observed here is similar to that observed for wild-type *L. pectinata* HbICN with some significant differences in the propionate and vinyl regions [21,22]. The main difference between the rHbICN PheB10Tyr and the wtHbICN (not shown) spectra is that for the former the 6-$H_{\alpha'}$ propionate peak appears as a downfield peak at 19.90 ppm, while for the latter this is an upfield peak present at 17.25 ppm. Likewise, the 2-H_α vinyl peak for rHbICN PheB10Tyr appears very downfield shifted at 19.40 ppm while for wtHbICN this is an upfield peak present at 17.07 ppm.

Fig. 2 shows the results of a variable temperature study that facilitated the assignment of the hyperfine shifted resonances, as illustrated on the insets under the diamagnetic envelope. As observed here, the His/CN^- axial-ligand interaction in the heme pocket reflects narrowest lines and large magnetic anisotropy in the NMR spectra, indicating that the quality of the ^{1}H-NMR spectra of low-spin ferrihemoproteins strongly depends on the axial ligands [1]. In the wtHbICN complex from *L. pectinata* the 6-propionate protons were assigned as follow: CαH at 5.70 ppm, $C_{\alpha'}H$ at 17.25 ppm, $C_\beta H$ at 0.13 ppm and $C_{\beta'}H$ at −1.20 ppm. Also, the 7-propionate protons were identified as CαH at 0.94 ppm, $C_{\alpha'}H$ at 2.08 ppm, $C_\beta H$ at −1.65 ppm and $C_{\beta'}H$ at 0.80 ppm [23]. These data together with our results from the temperature dependent studies and the inversion-recovery experiments (not shown) of rHbICN PheB10Tyr, allow distinguishing between the 6-H_α at 7.23 ppm, 6-$H_{\alpha'}$ at 19.90 ppm, 6-H_β at 0.20 ppm, 6-$H_{\beta'}$ at −1.40 ppm and 7-H_β at −1.30 ppm propionate protons as shown in Fig. 2. In addition, the major NOEs upon saturating the γ-meso shift at 5.15 ppm in the inversion-recovery spectrum of the rHbICN PheB10Tyr, suggest strong connections with the α and β protons of the 6-propionate group as predicted for the mean pyrrole H/CH_3 and meso-H shifts [1,24]. Heme-assignments deduced herein are compared with the paramagnetic systems of several hemoproteins with the standard Mb fold [20] and confirm the hyperfine shifts assignments for the rHbICN PheB10Tyr variant derivative. Fig. 3A shows a NOESY cross peaks map that reveals dipolar connectivities for the key distal residues TyrB10, GlnE7, and PheE11 present in the active center of the rHbICN PheB10Tyr mutant. These inter-residues patterns re-

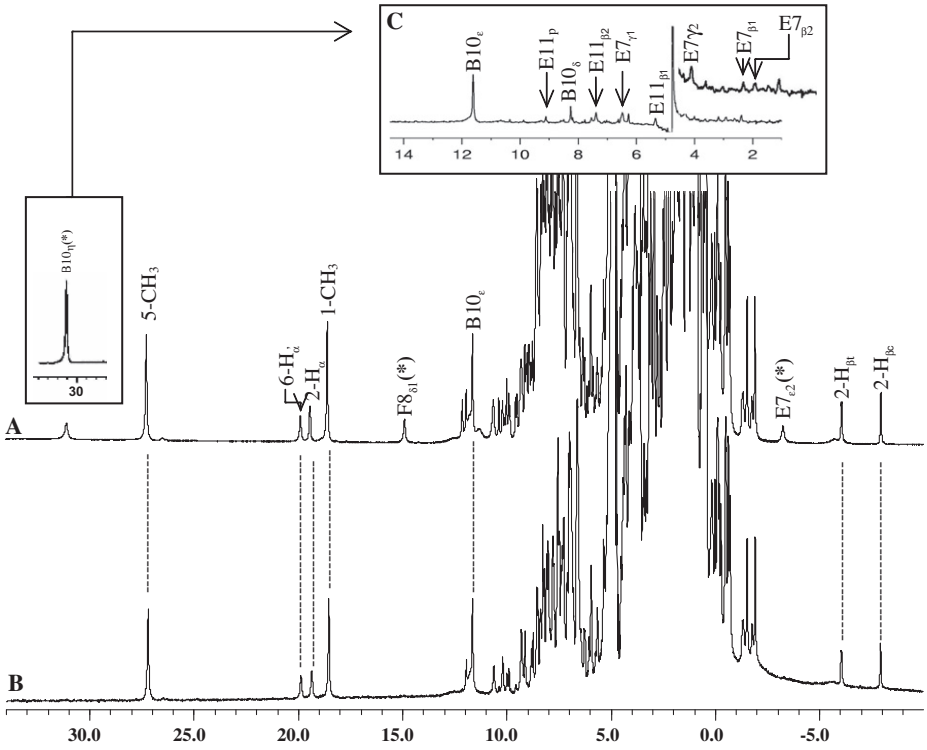

Fig. 1. 600 MHz ^{1}H-NMR spectra of rHbICN PheB10Tyr, pH 7.0, 25 °C. (A) ^1H_2O with saturation frequency at 31.00 ppm in the inset. (B) ^2H_2O solvent. (C) 1D NOE spectrum upon saturation of the TyrB10OH$_\eta$ peak in ^1H_2O. Labeled signals include heme signals in Fisher Notation (i.e., 1–CH_3, 6H$_{\alpha'}$) and amino acid signals in the helix position (i.e., B10$_\eta$ = Tyr29 ring OH$_\eta$; B10$_\varepsilon$ = Tyr29 ring C$_\varepsilon$H; E7$_{\varepsilon2}$ = Gln64 N$_{\varepsilon2}$H; F8$_{\delta1}$ = His96 imidazole N$_{\delta1}$H). Labile protons signals are identified with an asterisk (∗).

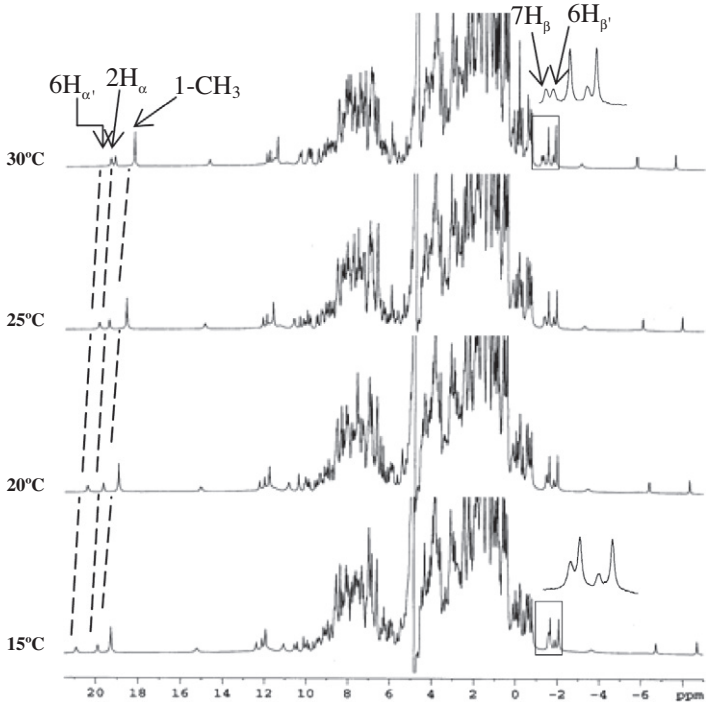

Fig. 2. Temperature dependence of the 600-MHz ^{1}H-NMR spectrum of rHbICN PheB10Tyr at pH 7.0 in ^1H_2O. The increasing hyperfine shift resolution for the propionate protons signals are illustrated in the up-field region, 0.00 to −4.00 ppm, at the temperature increase due to Curie relaxation. The variable temperature spectrum was observed in the range of 15–30 °C with increments of 5 °C between each one.

veal strong coupling when the PheB10Tyr single point mutation is introduced into the rHbICN active site. The intra-residue NOESY cross peak for the GlnE7 is clearly detected in the upper-field portion of the diagonal. Resonances for the GlnE7 side chain were located and assigned together with the characteristic pattern of TOCSY contacts and major NOEs connections with GlnE7 N$_{\varepsilon2}$H in

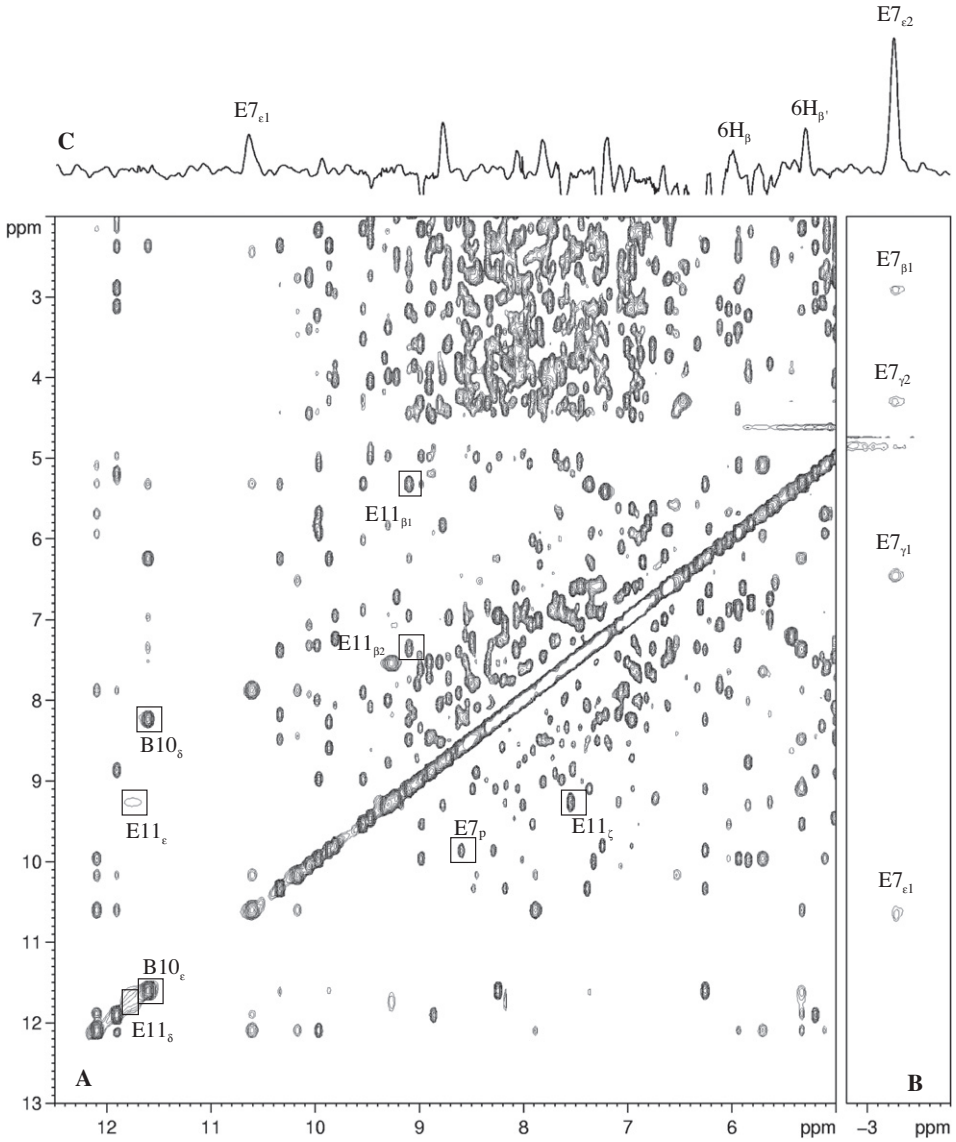

Fig. 3. A 2D ^{1}H-^{1}H NOESY (80 ms mixing time) at pH 7.0, 25 °C in $^{1}H_2O$ showing the (A) coupling between the TyrB10, GlnE7, and PheE11 spin systems; (B) NOEs observed in the GlnE7 side chain; (C) Majors NOEs detected in the 1D slice of NOESY corresponding to coupling with GlnE7 $N_{\varepsilon 2}H$.

a diamagnetic window ranging from 13.00 to −4.00 ppm (Fig. 3B and C). The 1D portion of one slice NOESY (Fig. 3C) at −3.27 ppm locates the strong to moderate dipolar contact between the GlnE7 - $N_{\varepsilon 2}H$ with the 6-H_{β} at 0.20 ppm and the 6-$H_{\beta'}$ at −1.40 ppm.

Overall, Table 1 summarizes the ^{1}H-NMR results obtained for rHbICN PheB10Tyr showing the distal residues rearrangement when compared to the wtHbICN complex. The significant changes in hyperfine chemical shifts, such as the 10.66 ppm for GlnE7 $N_{\varepsilon 1}H$ and −3.27 ppm for GlnE7 $N_{\varepsilon 2}H$ in the rHbICN PheB10Tyr mutant compared to the 14.05 ppm for GlnE7 $N_{\varepsilon 1}H$ and −1.39 ppm for GlnE7 $N_{\varepsilon 2}H$ in the wtHbICN complex, reveal that a conformational effect results when Phe is substituted by Tyr in the B10 position. For example, the side chain GlnE7NH_2-CO is shifted ($\Delta\delta = \delta_{\text{wild type}} - \delta_{\text{mutant}}$) upfield with $\Delta\delta = 3.39$ and $\Delta\delta = 1.88$ ppm near to the 6-propionate from its native structural position. In addition, comparison of ^{1}H-NMR of wtHbI [21,25] and the recombinant PheB10Tyr mutant cyanomet complexes reveals rotation about the 6-propionate CH_{α}–C_{pyrole} bond of the heme in the rHbICN PheB10Tyr heme pocket. Thus, differences in the chemical shifts corresponding to the alpha protons ($H_{\alpha}H_{\alpha'}$) and beta protons ($H_{\beta}/H_{\beta'}$) of the 6-propionate group are expected.

4. Discussion

The ^{1}H-NMR spectrum of rHbICN PheB10Tyr confirms a strong downfield shift for the 6-$H_{\alpha}H_{\alpha'}$ propionate with peaks at 7.23 and 19.90 ppm. Saturation transfer between amide, $N_{\varepsilon 2}H$, in the GlnE7 distal residue in rHbICN PheB10Tyr reveals strong and moderate NOEs connections with the 6-propionate $C_{\beta}H/C_{\beta'}H$, respectively. The structural behavior of the distal residues and the heme group in the active center was established by the NOESY cross-peak and NOE patterns including the paramagnetic relaxation properties, distinctive of the heme iron with 6th coordinate cyanide axial ligand [1]. The interactions that involve the peripheral groups in the heme via NOE showed a stable contribution in the rHbICN PheB10Tyr moiety. Regarding this, structural changes are revealed throughout major NOEs connections of the TyrB10$O_{\eta}H$ at 31.00 ppm with GlnE7$C_{\gamma 1}H/C_{\gamma 2}H$ at 6.46/4.31 ppm and PheE11$C_{\beta 1}H/C_{\beta 2}H$ at 5.33/7.36 ppm. Fig. 4 shows a schematic that describes the heme cavity in *L. pectinata* rHbICN PheB10Tyr mutant with the distal residues in contact with the heme, using iron-centered reference coordinate system (x′, y′, z′) for a porphyrin and defines the orientation of the axial His plane by the position of helices

Table 1
Comparison of ^{1}H-NMR chemical shifts of the B10, E7 and E11 distal amino acid residues in rHbICN PheB10Tyr mutant and wtHbICN from *Lucina pectinata*. (-) not observed. Bold values represent strongly shifted hyperfine resonance lines.

Residues	Protons	Chemical shifts (ppm)[a]	
		rHbICN PheB10Tyr	wtHbICN[b,c]
Tyr^{29}(B10)	N_pH	8.54	–
	$C_\alpha H$	4.30	–
	$C_{\beta1}H$	3.43	–
	$C_{\beta2}H$	3.63	–
	$C_\delta Hs$	8.22	8.70
	$C_\varepsilon Hs$	11.60	13.07
	$C_\zeta H$	–	18.77
	$O_\eta H$	**31.00**	–
Gln^{64}(E7)	N_pH	8.59	8.93
	$C_\alpha H$	3.98	4.62
	$C_{\beta1}H$	2.90	3.03
	$C_{\beta2}H$	2.60	3.29
	$C_{\gamma1}H$	6.46	7.63 (7.47)
	$C_{\gamma2}H$	4.31	4.97 (4.90)
	$N_{\varepsilon1}H$	**10.66**	**14.05 (13.80)**
	$N_{\varepsilon2}H$	**−3.27**	**−1.39 (−1.40)**
Phe^{68}(E11)	N_pH	9.09	9.89
	$C_\alpha H$	3.18	3.81
	$C_{\beta1}H$	**5.33**	**9.05**
	$C_{\beta2}H$	7.36	6.40
	$C_\delta Hs$	**11.75**	**7.47**
	$C_\varepsilon Hs$	**9.26**	**7.53**
	$C_\zeta H$	7.53	7.87

[a] Chemical shifts in ppm at 25 °C, pH 7.0 (rHbICN PheB10Tyr) and pH 7.2 (wtHbICN).
[b] [21].
[c] [25].

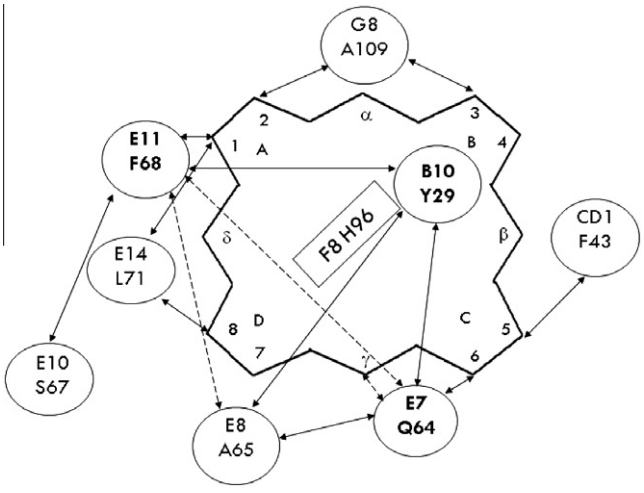

Fig. 4. Schematic representation of the distal heme pocket of rHbICN PheB10Tyr mutant showing major NOE dipolar contacts between distal residues (circles) and heme group. The NOEs connectivities are illustrated using double arrows where dashed (---) and solid (-) lines enclose the moderate and strong dipolar contacts, respectively. The heme group is located face-on view from the proximal side HisF8.

relative to the x′-axis [1]. As illustrated, the single PheB10Tyr mutation promotes a constrained heme pocket through structural conformational changes that include significant movements of the key distal side chains residues GlnE7 and PheE11 in the active center. A change in orientation is observed for GlnE7 as well as the 6-propionate group, which allows dipole interactions. Rotation of the heme 6-propionate group has also been observed in the photosynthetic cytochrome c_6 Q51 V variant from *Phormidium laminosum*, which showed that the axial Met ligand was stabilized through polar interactions with the imidazole and heme 6-propionate. The latter was possible owing to a 180° rotation of both heme propionates upon imidazole binding [26].

The detection of NOESY cross peaks between the $C_\delta H$ and the adjacent $C_\varepsilon H$ on the PheE11 aromatic ring at 11.75 and 9.26 ppm reveals strong displacement of the ring with respect to its native structure that have ring signals at 7.47 and 7.53 ppm [21]. Based on this, we suggest that the side chain of PheE11 swing 3.91 Å closed to the ligand in the heme pocket compared to the native HbICN complex as consequence of PheB10 substitution. Conserved residues such as PheCD1, AlaE8, LeuE14, AlaG8 and SerE10 are shown as probe for the sequence specific assignment through the NOE connectivities. These dipolar interactions in the distal cavity determine the geometry and properties of the active heme center for the rHbICN PheB10Tyr variant. Moreover, the X-ray crystal structure of the HbII-HbIII cyanide complex from *L. pectinata*, which has the same active center as rHbICN PheB10Tyr, shows that the 6-propionate and the GlnE7 residue have H-bonding orientation with distances between the 6-propionate Cβ and the GlnE7 $N_{\varepsilon2}$ of 4.37 Å in HbII chain A and 4.32 Å in HbIII chain B and between the 6-propionate Cβ and GlnE7$O_{\varepsilon1}$ of 3.49 Å in HbII chain A and 3.58 Å in HbIII chain B (data unpublished). Taken together, the results suggest that the dipolar contacts between the GlnE7 distal residue and the 6-propionate group are due to the tyrosine at the B10 position and that this residue is responsible for the new electrostatic interactions. Thus, a hydrogen bonding network is established in the distal region between the GlnE7 and 6-propionate group in rHbICN PheB10Tyr relative to the axial His plane, due to the electron withdrawing character of the hydrogen bonding, which contribute significantly to the modulation the heme iron electron density. This hydrogen bonding network loop between propionate, heme ligand and nearby amino acids support the fact that the heme reduction potentials are in part controlled by the interaction of the propionates and the nearby electronic environments [27].

Analyses of the resonance Raman spectra of deoxy, metcyano, carbonmonoxy, and oxy HbI derivatives have suggested the presence of moderate hydrogen bonding between Arg-99 and the heme-7-propionate. However, ^{1}H-NMR indicated that hydrogen bonding between the heme-6-propionate and amino acid residues is absent [28]. The flexibility of the heme-6-propionate observed in the rHbICN PheB10Tyr variant suggest that hemeproteins with the same electrostatic environment have the ability to induce a hydrogen bonding network loop between GlnE7, TyrB10, 6-propionate group, and the heme ligand. We suggest that for these systems the hydrogen bonding network may help to create a driving force that may modify the oxygen-heme reactivity, activate the heme chemical environment, and regulates the iron electron density of the heme, facilitating in turn oxygen metabolism. Hence, for *L. pectinata* HbII and HbIII as well as other trHbs this network might activate O_2 delivery and chemistry. Indeed, the X-ray crystal structure of the trHb from the green algae *Chlamydomonas eugametos* with cyanide as ligand (trHbC-CN^-) (PDB: 1DLY) strongly suggest H-bonding networks between GlnE7, TyrB10, 6-propionate group, and the bound ligand, which can modulate O_2 metabolism [29]. Analysis of the structure indicates distances for polar contacts between the 6-propionate C_β and the GlnE7 $N_{\varepsilon2}$ at 4.87 Å, the 6-propionate C_β and GlnE7$O_{\varepsilon1}$ at 4.15 Å, TyrB10O_η and GlnE7C_γ at 3.44 Å, and TyrB10O_η and CN at 2.36 Å [30]. Similarly, a sperm whale myoglobin mutant having GlnE7 and TyrB10(PDB: 1F63) and the hemoglobin from *Ascaris suum* (PDB: 1ASH), which naturally bears these two residues at the distal site show distances between the heme 6-propionate and nearby residues that can induce the H-bonding network mentioned above [31]. For instance, in the Mb mutant, designated to mimic the distal pocket of oxy-*Ascaris suum* Hb, possible hydrogen bonding interactions between 6-propionate C_β and the GlnE7 $N_{\varepsilon2}$, 6-propionate C_β and GlnE7$O_{\varepsilon1}$, and

TyrB10O_η and GlnE7C_γ are observed with X-ray distance of 4.54, 3.63, and 4.10 Å, respectively [32,33]. It is important to mention that the reactivity and affinity of these proteins for O_2 have been attributed to the H-bonding network between the TyrB10/GlnE7 pair. However, as we have shown interactions of this pair with flexible propionates groups should also be taken into account when analyzing the metabolism of O_2 with these proteins.

Acknowledgments

This work was supported by funds from the NSF (Grant 0843608) and NIH-NIGMS/MBRS-SCORE 5 S06GM008103-36. Special thanks to Dr. Gerd N. La Mar for his motivation on NMR of hemoproteins. We also thank Dr. Jeffrey S. De Ropp for the NMR facilities in the University of California at Davis, Dr. Vasyl Bondarenko for assistance with NMR experiments, Dr. Ruth Pietri for helpful suggestions and Dr. Carmen Cadilla for the construction of the rHbI mutant.

References

[1] G.N. La Mar, J.D. Satterlee, J.S. De Ropp, Nuclear Magnetic Resonance of Hemeproteins. in: K.M.S.K.M. Kadish, R. Guilard, (Ed.), The Porphyrin Handbook, Academic Press, 2000, pp. 185–298.
[2] V. Guallar, B. Olsen, The role of the heme propionates in heme biochemistry, J. Inorg. Biochem. 100 (2006) 755–760.
[3] R.E. Weber, S.N. Vinogradov, Nonvertebrate hemoglobins: functions and molecular adaptations, Physiol. Rev. 81 (2001) 569–628.
[4] Y. Gao, S.F. El-Mashtoly, B. Pal, T. Hayashi, K. Harada, T. Kitagawa, Pathway of information transmission from heme to protein upon ligand binding/dissociation in myoglobin revealed by UV resonance Raman spectroscopy, J. Biol. Chem. 281 (2006) 24637–24646.
[5] S. Schneider, J. Marles-Wright, K.H. Sharp, M. Paoli, Diversity and conservation of interactions for binding heme, Nat. Prod. Rep. 24 (2007) 621–630.
[6] T. Hayashi, K. Harada, K. Sakurai, H. Shimada, S. Hirota, A role of the heme-7-propionate side chain in cytochrome P450cam as a gate for regulating the access of water molecules to the substrate-binding site, J. Am. Chem. Soc. 131 (2009) 1398–1400.
[7] D.W. Kraus, J.B. Wittenberg, Hemoglobins of the *Lucina pectinata*/bacteria symbiosis I. Molecular properties, kinetics and equilibria of reactions with ligands, J. Biol. Chem. 265 (1990) 16043–16053.
[8] K.R.H. Read, The Hemoglobin of the Bivalve Mollusc *Phacoides pectinatus*, Gmelin. Bio. Bull. 123 (1962) 605–617.
[9] M. Rizzi, J.B. Wittenberg, A. Coda, M. Fasano, P. Ascenzi, M. Bolognesi, Structure of the sulfide-reactive hemoglobin I from the Clam *Lucina pectinata*, J. Mol. Biol. 244 (1994) 86.
[10] R. Pietri, A. Lewis, R.G. Leon, G. Casabona, L. Kiger, S.R. Yeh, S. Fernandez-Alberti, M.C. Marden, C.L. Cadilla, J. Lopez-Garriga, Factors controlling the reactivity of hydrogen sulfide with hemeproteins, Biochemistry 48 (2009) 4881–4894.
[11] R. Pietri, L. Granell, A. Cruz, W. De Jesus, A. Lewis, R. Leon, C.L. Cadilla, J. Lopez-Garriga, Tyrosine B10 and heme-ligand interactions of *Lucina pectinata* hemoglobin II:control of heme reactivity, Biochimi. Biophys. Acta 1747 (2005) 195–203.
[12] H. Ouellet, L. Juszczak, D. Dantsker, U. Samuni, Y.H. Ouellet, P. Savard, J.B. Wittenberg, B.A. Wittenberg, J.M. Friedman, M. Guertin, Reactions of *mycobacterium tuberculosis* truncated hemoglobin O with ligands reveal a novel ligand-inclusive hydrogen bond network, Biochemistry 42 (2003) 5764–5774.
[13] H. Ouellet, Y.H. Ouellet, C. Richard, M. Labarre, B.A. Wittenberg, J.B. Wittenberg, M. Guertin, Truncated hemoglobin HbN protects *mycobacterium bovis* from nitric oxide, Proc. Natl. Acad. Sci. 99 (2002) 5902–5907.
[14] E.S. Peterson, S. Huang, J. Wang, L.M. Miller, G. Vidugiris, A.P. Kloek, D.E. Goldberg, M.R. Chance, J.B. Wittenberg, J.M. Friedman, A comparison of functional and structural consequences of the tyrosine B10 and glutamine E7 mofits in two invertebrate hemoglobins (*Ascaris suum* and *Lucina pectinata*), Biochemistry 36 (1997) 13110–13121.
[15] J.A. Gavira, A. Camara-Artigas, W. De Jesus-Bonilla, J. Lopez-Garriga, A. Lewis, R. Pietri, S.R. Yeh, C.L. Cadilla, J.M. Garcia-Ruiz, Structure and ligand selection of hemoglobin II from *Lucina pectinata*, J. Biol. Chem. 283 (2008) 9414–9423.
[16] T. Hayashi, T. Matsuo, Y. Hitomi, K. Okawa, A. Suzuki, Y. Shiro, T. Iizuka, Y. Hisaeda, H. Ogoshi, Contribution of heme-propionate side chains to structure and function of myoglobin: chemical approach by artificially created prosthetic group, J. Inorg. Biochem. 91 (2002) 94–100.
[17] R.G. Leon, H. Munier-Lehmann, O. Barzu, V. Baudin-Creuza, R. Pietri, J. Lopez-Garriga, C.L. Cadilla, High-level production of recombinant sulfide-reactive hemoglobin I from *Lucina pectinata* in *Escherichia coli*: high yields of fully functional holoprotein synthesis in the BLi5 *E. coli* strain, Protein Expr. Purif. 38 (2004) 184–195.
[18] J. Cerda, Y. Echevarria, E. Morales, J. Lopez-Garriga, Resonance Raman studies of the heme–ligand active site of hemoglobin I from *Lucina pectinata*, Biospectroscopy 5 (1999) 289–301.
[19] D.W. Kraus, J.B. Wittenberg, Hemoglobins of the *Lucina pectinata*/bacteria symbiosis: II. An electron paramagnetic resonance and optical spectral study of the ferric proteins, J. Biol. Chem. 265 (1990) 16054–16059.
[20] S.D. Emerson, G.N. La Mar, Solution structural characterization of cyanometmyoglobin: resonance assignment of heme cavity residues by two-dimensional NMR, Biochemistry 29 (1990) 1545–1556.
[21] B.D. Nguyen, X. Zhao, K. Vyas, G.N. La Mar, R. Ashley Lile, E.A. Brucker, G.N. Phillips, J.S. Olson, J.B. Wittenberg, Solution and crystal structures of a sperm whale myoglobin triple mutant that mimics the sulfide-binding hemoglobin from *Lucina pectinata*, J. Biol. Chem. 273 (1998) 9517–9526.
[22] J.F. Cerda-Colon, E. Silfa, J. Lopez-Garriga, Unusual rocking freedom of the heme in the hydrogen sulfide-binding hemoglobin from *Lucina pectinata*, J. Am. Chem. Soc. 120 (1998) 9312–9317.
[23] X. Zhao, Solution structure determination of *Lucina pectinata* hemoglobin I and sperm whale myoglobin mutants, Department of Chemistry, University of California, Davis, 1994, pp. 474.
[24] G.N. La Mar, Model compounds as aids in interpreting NMR spectra of hemoproteins, in: R.G. Shulman (Ed.), In Biological Application of Magnetic Resonance, Academic Press, New York, 1979, pp. 305–341.
[25] B.J. Ramos-Santana, A nuclear magnetic resonance investigation of the influence of distal glutamine on structural properties of *Lucina pectinata* Hemoglobin I, Department of Chemistry, University of Puerto Rico, Mayaguez, 2003, pp. 78.
[26] B.S. Rajagopal, M.T. Wilson, D.S. Bendall, C.J. Howe, J.A.R. Worrall, Structural and kinetic studies of imidazole binding to two members of the *cytochrome c6* family reveal an important role for a conserved heme pocket residue, J. Biol. Inorg. Chem. 16 (2011) 577–588.
[27] J.J. Warren, J.M. Mayer, Proton-coupled electron transfer reactions at a heme-propionate in an iron-protoporphyrin-IX, J. Am. Chem. Soc. 133 (2011) 8544–8551.
[28] E. Silfa, M. Almeida, J. Cerda., S. Wu, J. López -Garriga, Structural characterization and dynamics events in hemoglobin I from *Lucina pectinata*: Unusual conformation of propionates and vinyl's heme peripheral groups. Spectrosc. Biol. Mol. Trends (1997) 79–80.
[29] T. Egawa, Syun-Ru Yeh, Structural and fuctional properties of hemoglobins from unicellular organisms as revealed by resonance Raman spectroscopy, J. Inorg. Biochem. 99 (2005) 72–96.
[30] A. Pesce, M. Couture, S. Dewilde, M. Guertin, K. Yamauchi, P. Ascenzi, L. Moens, M. Bolognesi, X-Ray crystal structure of hemoglobin from the green unicelluar alga *Chlamydomonas eugametos*, EMBO J. 19 (2000) 2424–2434.
[31] W. Zhang, F. Cutruzzola, C. Travaglini-Allocatelli, M. Brunori, G.N. La Mar, A myoglobin mutant designed to mimic the oxygen-avid *Ascaris suum* hemoglobin: elucidation of the distal hydrogen bonding network by solution NMR, Biophys. J. 73 (1997) 1019–1030.
[32] M. Brunori, F. Cutruzzola, C. Savino, C. Travaglini-Allocatelli, B. Vallone, Q.H. Gibson, Crystal structure of deoxy sperm whale myoglobin mutant Y(B10)Q(E7)R(E10), Biophys. J. 76 (1999) 1259–1269.
[33] J. Yang, A.P. Kloek, D.E. Goldberg, F.S. Mathews, The structure of *Ascaris* hemoglobin domain I at 2.2 A resolution: molecular features of oxygen avidity, Proc. Natl. Acad. Sci. USA 92 (1995) 4224–4228.